

SESSION E:
SINGLE-EVENT PHENOMENA

PLASMA SCREENING OF FUNNEL FIELDS*

R. M. Gilbert, G. K. Ovrebo, and J. Schifano
 Harry Diamond Laboratories
 Adelphi, MD 20783

ABSTRACT

A plasma screening factor has been added to the McLean-Oldham effective funnel length model. Based on the skin depth concept, the factor is intended to provide for plasma screening of funnel fields in heavy-ion tracks crossing reverse-biased silicon and gallium arsenide junctions. Comparisons between screened-funnel predictions of prompt charge collection and experimental data show improved predictive accuracy at low and intermediate values of junction bias.

INTRODUCTION

The funnel effect refers to a depletion-layer field distortion that occurs along the tracks of ions penetrating reverse-biased junctions. It was first identified by Hsieh, Murley, and O'Brien.¹⁻³ Using experiments and computer models, they studied charge collection mechanisms in semiconductor junctions struck by 5-MeV alpha particles. They reported that charge carriers in the high-field region near the pn junction caused the depletion-layer field to momentarily extend down the track into the previously field-free region. The result was a significant increase in the amount of ionization charge collected by electric-field drift. This process is very rapid, typically lasting less than a nanosecond for the junction biases and doping levels of interest. Accordingly, Hsieh and his coworkers concluded that the funnel mechanism made single-event upset (SEU) a more serious threat to semiconductor devices than had been believed.

Several researchers have worked to quantify the funnel effect using simple, approximate, analytical models. They are Hu,⁴ Messenger,⁵ and the team of McLean and Oldham.⁶ Of these three, only the McLean-Oldham effective funnel length model has been compared to heavy-ion data. On the first occasion, Oldham and McLean compared their model to data taken on silicon diodes.⁷ In addition to alpha particles, they bombarded their test diodes with beryllium, oxygen, silicon, and copper ions. For junction biases higher than about 5 V and ions heavier than beryllium, their funnel model predicted 100-percent drift collection of the ionization charge produced. The corresponding measurements showed that funneling was a strong effect, giving factor-of-two and three enhancements over the depletion-layer contribution. However, the total drift collection was significantly less than 100 percent until biases exceeded about 15 V. They attributed this discrepancy to the dense ionization and high conductivity in heavy-ion tracks. They suggested that in these cases their model's value for the average collection field, V_0/L_c , was excessive, that the highly conducting plasma columns would actually support a much smaller potential gradient, and that the balance of the potential drop would fall across the non-ionized region beyond the end of the track.

A second comparison between the McLean-Oldham model and heavy-ion data was made by Gilbert et al.⁸ They compared model predictions to data taken with alpha particles, oxygen, chlorine, and copper ions bombarding n-type gallium arsenide Schottky-barrier diodes. Their results were similar to the Oldham-

McLean comparisons in that the model predicted 100-percent drift collection for heavy ions and biases above a few volts, while the measurements showed only a 10 to 30-percent funnel enhancement over the depletion-layer contribution.

The purpose of this paper is to provide an empirical adjustment to the McLean-Oldham model to account for the heavy-ion case. Our approach is to use a simple phenomenological representation of electric field screening based on the skin depth concept. This representation yields a simple correction factor to account for the reduced drift collection in densely ionized tracks.

THEORY

In the discussion below, several conditions are assumed to apply: (1) The time required for the bias circuit to replace collected charge on the junction is long compared to the duration of drift collection. (2) The lateral dimensions of the diode are sufficiently large that the bias charge on the junction is much greater than the free charge produced in the ion track; thus, the charge collection that follows the ion strike does not substantially alter the potential difference across the junction and the overall field distribution. (3) Dark current is negligible compared to all other currents in the problem. These conditions apply to the heavy-ion experiments referenced in this paper.

Given these conditions, we first offer a phenomenological description of the charge-funneling mechanism in the light-ion track, and then follow with a description of plasma screening of the funnel-field in a very heavily ionized track. Figure 1 shows the track of a light ion (e.g., alpha particle) perpendicular to the plane of the junction. A reverse-biased p^+n Schottky-barrier diode is depicted. After the initial track ionization is thermalized, a process that occurs in times of the order of 10^{-12} s and leaves the track with a radius of about $0.1 \mu m$,³ the initial carrier transport effects include the following: (1) The plasma column in the depletion layer is polarized almost instantly (about as fast as it is created), excluding the positive donor charge in its interior. This charge "surfaces" at the junction and recombines with an equal negative charge on the electrode. The neutralization of this track volume results in an unbalanced radial field component in the depletion layer directed in towards the track axis. (2) Ionization electrons in the same part of the track are attracted by the surrounding charged donors (i.e., they respond to the radial field component) and drift radially outward into the depletion layer, neutralizing charged donors there. (3) Ionization holes produced in the depletion layer are attracted to the negatively charged metal contact layer. (4) On a much slower time scale, the column begins a relatively slow expansion as ambipolar diffusion takes place. In this early phase, most of the electrons leaving the track come from that segment lying in the original depletion layer; carriers well beyond the depletion layer initially see no field and are not affected. In this and subsequent phases of charge collection, rates of hole collection at the surface and the radial drift of electrons out of the track are approximately equal, so that the track plasma remains essentially neutral inside its sheath.⁶ The sheath is the exterior layer of the plasma column where electrons leave the neutral

* Work jointly sponsored by Ballistic Missile Defense Systems Command, Huntsville, AL, and Defense Nuclear Agency, Washington, DC 20305.

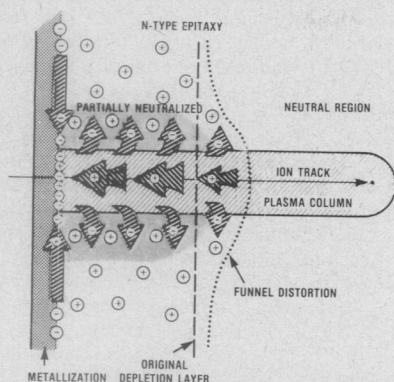


Fig. 1 Charge-carrier motions following an ion strike on a reverse-biased p^+n Schottky-barrier diode.

plasma under the influence of radial fields. Funneling occurs as this electron space charge "fans out" and neutralizes part of the positively charged donor distribution in the vicinity of the track (a process that takes tens of ps). Some of the field lines associated with local electron charges on the metallization then no longer terminate on charged donors in the original depletion layer, but instead extend into the formerly neutral region. Alternatively, one may picture the majority carriers that have left the column as creating their own additional depletion volume in what was initially neutral space. The result is a bulge on the original depletion layer centered on the track. Track electrons there are then subjected to a radial field and are pulled out of the plasma as their hole counterparts are funneled up the track toward the surface. The resulting increase in space charge further extends the bulge. The consequence of this cause-and-effect cycle is an extension of a longitudinal field up the track into the initially neutral region and a resulting increase in prompt (drift) charge collection over and above that provided by charge in the original depletion layer.

Conservation of current in this transiently isolated junction requires a local closure of current paths. The charge motions described in figure 1 define the closed conventional-current loop shown in figure 2a: a radial "fan-out" of electron current out of the track into the depletion layer, a hole current up the track and across the junction, a radial inward-directed electron replacement current on the electrode, and, closing the loop, a displacement current normal to the junction. This last current segment is the relatively small time-rate-of-change of the electric displacement D in the depletion layer due to the partial neutralization of charge on the junction, integrated over the area of the diode ($\partial D/\partial t$ is directed opposite to D .) The diode current paths drawn in 2a suggest a simple analogy, which we show in figure 2b. Here, two oppositely charged metal plates are suddenly shorted by a long nail, which represents the heavy-ion track. This analogy cannot provide for either the discharge-limiting effects of the Schottky barrier, the depletion-layer bulge (the funnel), or the hole current in the ion track. Nevertheless, the picture gives a good representation of the closed SEU current loops in large diodes transiently isolated from their bias circuitry; it shows how the electric field in the nail would be largely confined to that current-carrying portion lying between the two charge layers, rather than to the tip of the nail. In the diode, as the last of the drift and diffusion charge is collected, the depletion region is reestablished as a uniform, slightly thinner layer across the entire diode area, and the potential difference across the

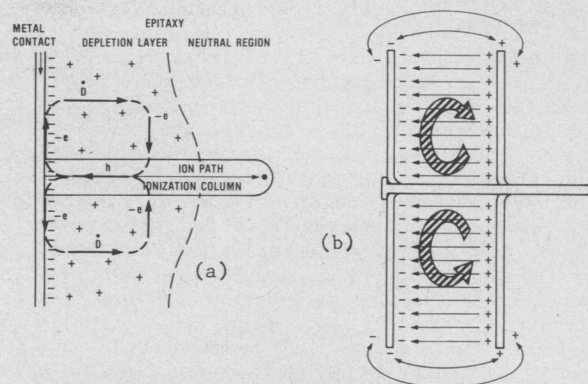


Fig. 2 Arrows denote closed conventional current paths: (a) large diode and (b) a parallel-plate analogy.

junction settles at the original value minus Q/C , the ionization-charge collected divided by the junction capacitance. In due course, this voltage drop produces an appropriate electron current in the bias-circuit loop, which includes the substrate, the missing (recombined) charge on the junction is replaced, and the full junction bias is restored.

In contrast to the large-area diode depicted above, integrated circuits, especially large- and very-large-scale integrated circuits, have extremely small junction areas and capacitances. In such devices, the collection of even a portion of the ionization charge in the ion track may be sufficient to neutralize all the charge on the reverse-biased junction, causing a complete collapse of the depletion layer and changes of state in nearby circuit elements. The additional complexity of this problem is outside the scope of the present work, and will not be discussed further here.

If the first condition given above does not apply, and charge is replaced on the junction as fast as it is collected, then a prompt field is produced directly across the active and substrate layers lying between the diode contacts. Majority carriers stream out of the track into the substrate and are collected at the buried electrode. Their almost immediate presence along the whole length of the track creates a much more direct and rapid growth of funneling than we show in figure 1. One would then expect a weaker longitudinal electric field along the full length of the track, and a much stronger field at its tip. This would be analogous to the plate on the right side of figure 2b being re-identified as the buried contact and the nail (track) being shortened so that it reaches only a short distance into the space between the plates. In the diode, the field (and the currents that follow it) would spread and thin from the end of the track on toward the substrate electrode, following the spreading resistance as described qualitatively by Messenger.⁵ Grubin, et al,⁹ have modeled this problem with a finite difference computer code similar to that used by Hsieh et al.² They held their n^+p junction at constant bias through the event (this is equivalent to an assumption of instantaneous replacement of the collected charge), and calculated time-dependent currents through the substrate, i.e., across the diode contacts. They concluded that these currents are more directly controlled by junction bias and the substrate parameters (resistivity, thickness, etc.) than by the details of the track geometry and density. Thus, if one is able to hold a junction bias constant through an ion strike, the basic response would be a fast-rising current in the diode circuit, rather than a

sudden potential drop across the diode junction followed by a relatively slow replacement of charge.

We suspect that most device biasing circuits will provide replacement charge in times much longer than the tenths of ns required for prompt-charge collection in single event upsets. For example, even a 15-cm battery supply loop has at least a 0.5-ns speed-of-light transit time; the effects of stray series inductance and shunt capacitance on the nominal bias loop impedance and larger bias loop dimensions can increase the charge replacement times even more, fulfill the second condition, and insure that funneling in the struck junction will follow the localized pattern given in figure 1. One might have to employ low-impedance transmission line techniques in the bias circuit to reduce charge replacement times to values close to prompt collection pulse widths. For the remainder of this discussion, we assume that all three conditions given earlier apply.

If the incident particle is now assumed to be a heavy ion, i.e., any ion heavier than beryllium, the ionization density is substantially greater than that in alpha particle tracks, and the drift charge collection predicted by the McLean-Oldham model is not fully realized. We suggest that the smaller collection may be explained by a plasma screening effect that prevents the full extension of the funnel field down the track into the neutral region. Figure 3 shows how the field, potential, and charge distributions might be altered by a plasma screening effect near the end of the funnel. As the funnel field begins to extend into the neutral part of the track, and carriers there are set in motion, a quasi-static shift in the charge distribution occurs, wherein minority-carrier holes (on time average) are brought closer to the electrode as electrons are pushed away from the electrode and separated radially. This time-averaged polarization shift of charge density screens the field--the termination of field lines on minority carriers is now accomplished closer to the surface--and carriers beyond do not see a collection field.

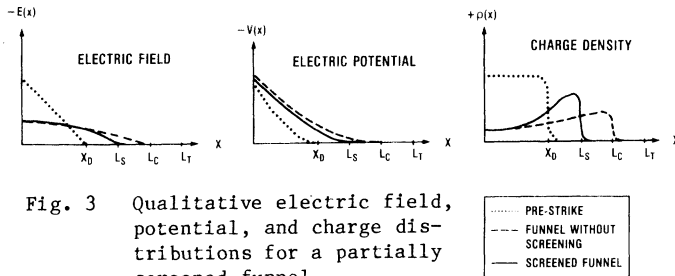


Fig. 3 Qualitative electric field, potential, and charge distributions for a partially screened funnel.

To devise a quantitative measure of this screening effect, we refer to the phenomenon of plane-wave attenuation in a conducting medium and the concept of skin depth. It is well-known that a plane wave is rapidly attenuated as it propagates into a good conductor. The attenuation factor f varies with propagation distance x according to:

$$f = e^{-\frac{x}{\delta}}, \quad \text{where } \delta \sim \sqrt{\frac{T}{\pi\mu\sigma}} \quad (1)$$

is the skin depth and T , μ , and σ are the plane wave period, the permeability of the target material, and its conductivity, respectively. Admittedly, the situation that exists in a semiconductor device after a heavy-ion strike differs from the case of the plane wave in a conductor: the electric field of the plane wave is transverse and oscillatory, while in the diode depletion layer, the electric funnel field is longitudinal and short-lived. Nevertheless, there is a similarity in the two situations that suggests the use

of an effective plasma attenuation factor of the form given above for the funnel field in the ion track. In both cases, free carriers move during a well-defined time interval to neutralize the field at their locations. In both cases, the extent of this neutralization is controlled by the conductivity and a critical time period. The greater the conductivity, the stronger the neutralization of fields and the shorter the distances into the two media that the fields can reach. Analogous to the plane-wave period T in (1), we choose the characteristic screening period to be the time it would take a minority carrier in the plasma column to drift to the surface from a maximum distance L . L is the length of track required to provide the quantity of charge predicted by the McLean-Oldham model; note that this is not that model's effective funnel length, L_c , which can exceed the track length for heavy, short-range particles. The screening period is then:

$$\tau \approx \frac{L}{\langle v_{mic} \rangle} \quad (2)$$

Here the average minority carrier drift velocity $\langle v_{mic} \rangle$ corresponds to an average field,

$$\langle E \rangle \approx \frac{1}{2} \frac{V_0}{L}, \quad (3)$$

where V_0 is the applied bias.

To complete the derivation of a screening factor, a characteristic length is needed. Since we used L to derive τ , and since the funnel field is assumed to collect charge from as far up the track as the distance L in the absence of screening, L is taken to be the representative unscreened field penetration depth. The result is an expression for an attenuation factor f_s due to screening given by

$$f_s = e^{-\frac{L}{\delta}}, \quad \text{with } \delta = \sqrt{\frac{\tau}{\pi\mu\sigma}} \quad (4)$$

In this expression, the permeability is taken to be that of free space, and the conductivity is the low-field limit of conductivity due to the initial hole and electron densities.

This reduction factor is now applied to the funnel contribution in the following expression for the total prompt charge Q_p :

$$Q_p = N_0 [x_D + f_s (L - x_D)]$$

where N_0 is the initial ionization line density and x_D is the initial depletion layer thickness. The justification for applying an electric field attenuation factor to a collection length is that the funnel portion of L is proportional to the electric field through the minority carrier drift velocity, at least for velocities significantly less than the saturation value (eq. (2), McLean and Oldham⁶).

This representation of the screening effect is an empirical one--we know that the McLean-Oldham funnel prediction is too high for heavy-ion tracks, and that experiments show prompt collection falling between the 100-percent prediction and the "zero-funnel" result (collection from just the original depletion-layer segment of the track). Since it is applied to just the funnel increment of collected charge, the screening factor developed above is bound to improve the prediction accuracy in the mid-range of diode biases for heavy ions. It remains to be demonstrated later in this report how well the treatment works overall, not just for the heavy-ion case, but also for the light-ion case, where plasma screening should be a small influence and the McLean-Oldham model is already quite accurate.

We offer a note on ionization recombination. In their investigation of charge collection in gallium arsenide diodes struck by alpha particles, Hopkins and Srour attributed a measured 15-percent shortfall in total charge collection to Auger and radiative recombinations.¹⁰ Based on this estimate, one would expect an even greater effect in the more strongly ionized tracks of heavy ions. Nevertheless, we do not attempt to include recombination in our computations here, for several reasons. First, the 15-percent shortfall reported by Hopkins and Srour is not a decisive margin in light of normal experimental uncertainties. Second, the heavy-ion data we use to evaluate our screening treatment did not provide a clear indication of recombination.^{8,11} Third, the Auger coefficients reported in the literature are scattered over 9 orders of magnitude;¹⁰ with that uncertainty, a meaningful evaluation of the importance of Auger recombination would be difficult. Fourth, radiative recombination produces photons, a good portion of which will be reabsorbed within $\sim 2 \mu\text{m}$, producing new electron-hole pairs.¹⁰ For these reabsorbed photons, the net effect of radiative recombination will be only a moderate diffusing of the plasma column. Last, it is not clear what influence funnel fields will have on the various recombination processes; one might expect that the non-equal momenta imparted to electrons and holes by the field would reduce recombination coefficients from published values, which are typically appropriate for field-free plasmas. For these reasons, we will not include recombination in our modeling study, but instead leave it as an undetermined parameter.

THE EXPERIMENT

As described in reference 8, the heavy-ion experiments on gallium arsenide were performed at the Rutgers University Tandem Vandegraaff Accelerator Facility; the alpha particle measurements were carried out at Harry Diamond Laboratories. Figures 4a, b, and c show the diode holder, the test circuit, and the laboratory setup in the accelerator facility, respectively. Ion beams produced by the accelerator were scattered through a thin gold foil (0.47 mg/cm^2) into a 20° side-drift tube. All diodes were exposed in vacuum to low ion count rates ($\sim 10/\text{s}$) to facilitate isolation of the single-event response. Ion beams were blocked between measurements to avoid excessive accumulation of damage in the diodes. This was a purely precautionary measure, and current-voltage characterizations performed on the test diodes after the experiments matched those made before beam exposures. Ion energies were calculated using Rutherford scattering kinematics and the Ziegler stopping powers.¹¹ Ion energies were also measured with an EG&G Ortec silicon surface-barrier detector calibrated in vacuum using ^{241}Am alpha particles. Differences between measured and calculated ion energies were between 1 and 2 percent. The drift and diffusion components of charge collection were measured with a Tektronix 6201 high-impedance probe as a function of reverse bias voltage in two sets of n-type gallium arsenide diodes with semiconducting substrates. Diode epi-layers were sulfur-doped to $1.3 \times 10^{15}/\text{cm}^3$ in one set, and to $8 \times 10^{14}/\text{cm}^3$ in the other. All gallium arsenide substrates were doped with tellurium to $3 \times 10^{18}/\text{cm}^3$. The signal-processing equipment was gain calibrated using n-type silicon diodes with very low doping ($9 \times 10^{13}/\text{cm}^3$), biased high enough to insure total charge collection. A Tektronix 7104 1-GHz oscilloscope and camera were used to record charge-collection signals.

The procedure followed in recording a gallium arsenide diode response under given bias and beam conditions was to expose the diode to the beam with

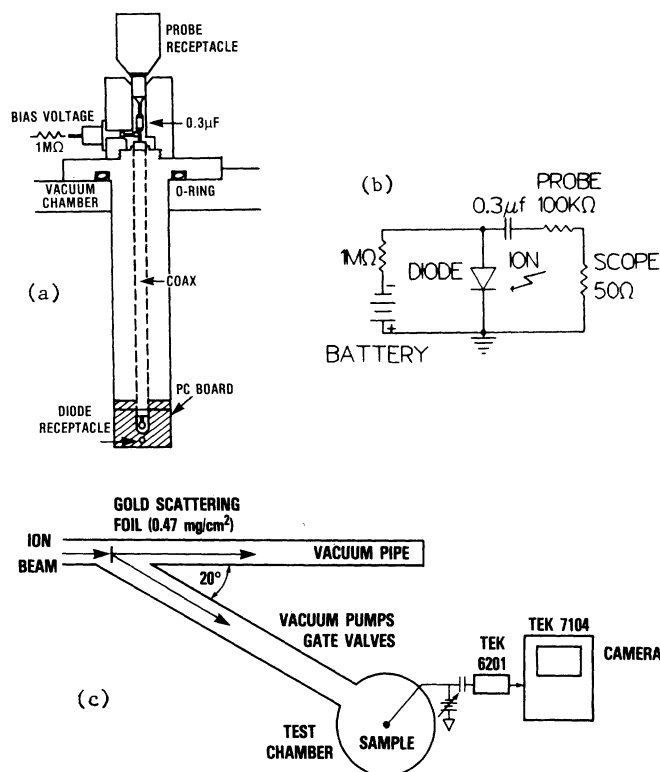


Fig. 4 Experimental configuration for heavy-ion measurements: (a) diode holder, (b) test circuit, and (c) laboratory bay setup

the camera shutter held open for several seconds, or until the oscilloscope trigger indicator registered 10 to 20 strikes. The resulting multiple exposure on the film invariably showed a very well-defined trace, usually having about 3 or 4 times the single-trace thickness, a measure of the direct-hit signal variation. The film also typically showed a faint scattering of smaller-amplitude, slower-rising signals that we interpret as near misses. The peak prompt and final diode responses were taken from the center of the trace and were converted to collected charges using the measured diode and holder capacitances. These capacitance measurements were performed in-situ before and after the ion bombardments (pre- and post-exposure readings agreed to within 1 percent). Circular metallizations on the diode surfaces were made large, 1.0 mm diameter, to insure that the frequency dependence of the probe capacitance would be a small perturbation to the total capacitance charged by the ion strike. The nominal probe capacitance was 3 pF, with a frequency-dependent variation of $\sim 1 \text{ pF}$. By comparison, the zero-bias capacitances of the low- and highly-doped diodes, including an 8-pF holding fixture, were typically 90 and 125 pF, respectively; at -20 V , these diode-and-holder capacitances fell to about 27 and 32 pF, respectively.

RESULTS

Comparisons between predicted and measured charge collection in gallium arsenide are shown in figures 5 through 8 for alpha particles and oxygen, chlorine, and copper ions, respectively (see reference 8). The point-to-point amplitude variations shown in the data, each point of which represents an average of 10 to 20 responses, is unexplained, but was shown to be reproducible by repeating selected portions of the test sequence. The uncertainty bars reflect both the maximum variation in the direct hit signals recorded during the multiple exposure of the film and the uncertainty in averaging out high-frequency signal oscillations.

Legend for figures 5-10:

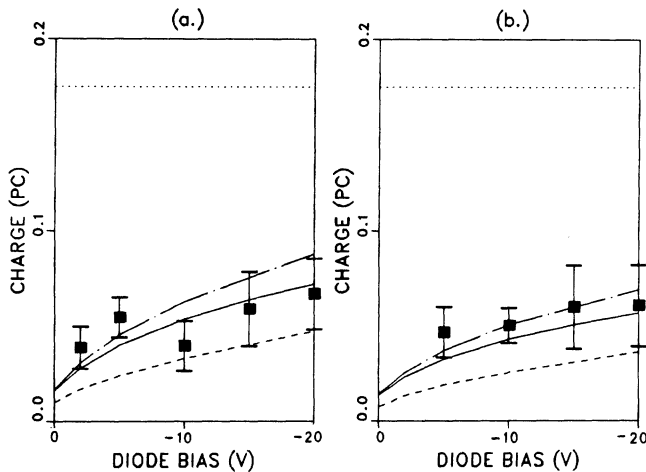
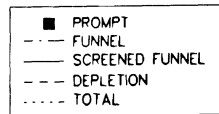


Fig. 5 5.2-MeV alpha particles in GaAs: (a) $N_D = 8.0 \times 10^{14}/\text{cm}^3$, (b) $N_D = 1.3 \times 10^{15}/\text{cm}^3$.

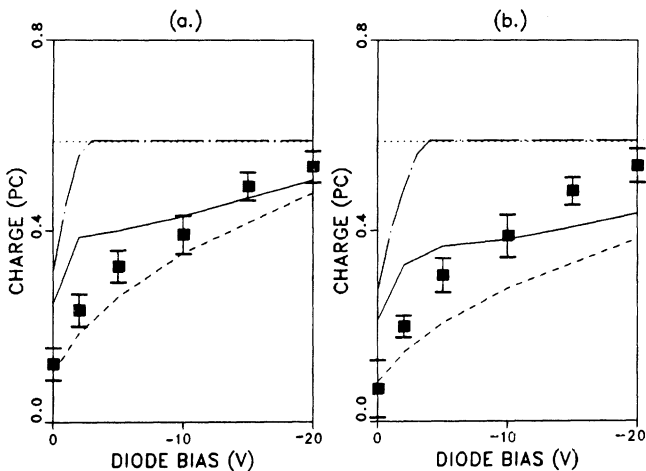


Fig. 6 17.7-MeV ^{16}O ions in GaAs: (a) $N_D = 8.0 \times 10^{14}/\text{cm}^3$, (b) $N_D = 1.3 \times 10^{15}/\text{cm}^3$.

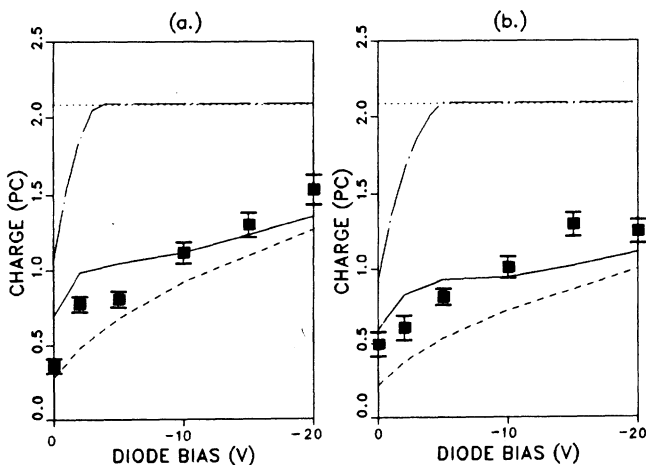


Fig. 7 62.5-MeV ^{35}Cl ions in GaAs: (a) $N_D = 8.0 \times 10^{14}/\text{cm}^3$, (b) $N_D = 1.3 \times 10^{15}/\text{cm}^3$.

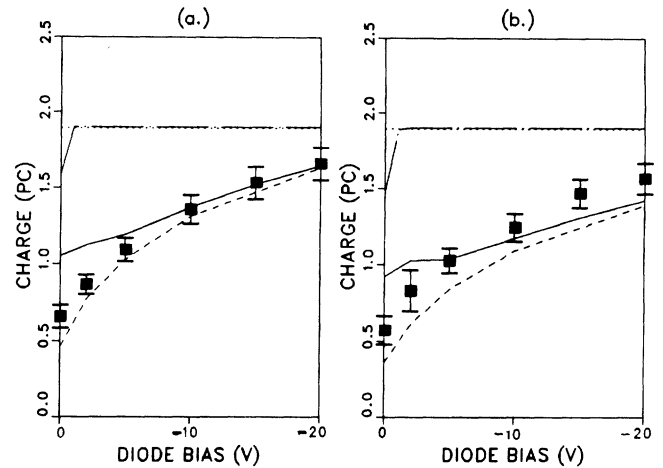


Fig. 8 56.9-MeV ^{63}Cu ions in GaAs: (a) $N_D = 8.0 \times 10^{14}/\text{cm}^3$, (b) $N_D = 1.3 \times 10^{15}/\text{cm}^3$.

Experimental measurements are matched with predictions taken from the McLean-Oldham effective funnel-length model (the dot-dash curves) and the plasma screening treatment (solid curves). Plasma screening as it has been modeled is seen to have only a modest effect on predictions for alpha particles as expected, giving results that still fall near the measured data. For the heavier ions, the screening effect is much more pronounced. Where the unscreened model predicts 100-percent drift collection at all biases above a few volts, the screened-funnel predictions fall considerably lower and much closer to the measurements. Compared to measured data, the screening treatment moderately overpredicts low-bias collection and understates collection at high bias.

Figures 9 and 10 show charge collection measurements made by Oldham and McLean in n-type silicon for alpha particles⁶ and copper ions, respectively. Measurements in each figure are accompanied by corresponding screened and unmodified funnel predictions. The performance of the screened-funnel treatment is much the same in silicon as in gallium arsenide--predictions for alpha particles are shifted down slightly from the funnel predictions, and the collection for copper ions is moderately overstated at low bias and understated at higher biases relative to the measured data. In figure 10, the screened funnel predictions also show a negative slope at intermediate biases. This effect derives from the application of the screening factor to just the funneled portion of the

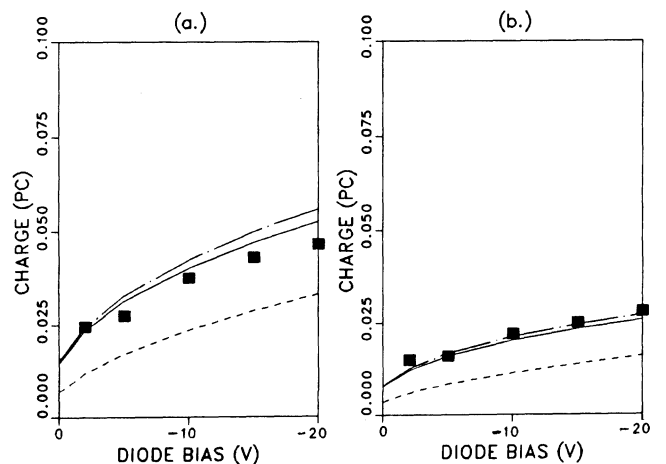


Fig. 9 5.2-MeV alpha particles in n-type Si: (a) $N_D = 1.0 \times 10^{15}/\text{cm}^3$, (b) $N_D = 4.0 \times 10^{15}/\text{cm}^3$.

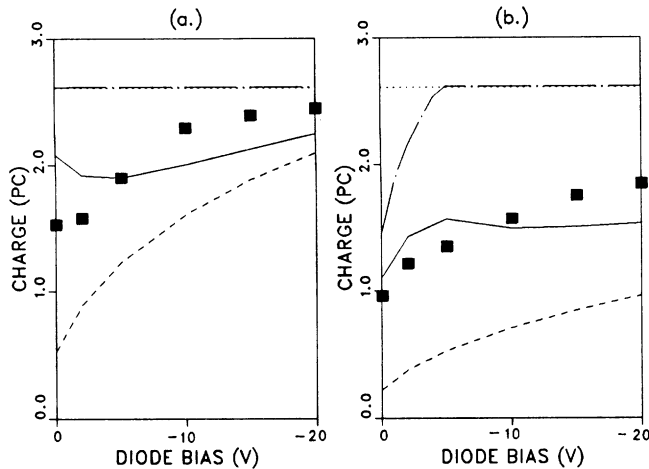


Fig. 10 59.6-MeV ^{63}Cu ions in n-type Si: (a) $N_D = 4.7 \times 10^{14}/\text{cm}^3$, (b) $N_D = 2.8 \times 10^{15}/\text{cm}^3$.

prompt charge predicted by the McLean-Oldham model. At these biases, the decrease in this product more than offsets the calculated increase in the depletion-layer contribution. The overall result of the treatment, nevertheless, is an improvement in the prediction accuracy for silicon as well as gallium arsenide.

It is also significant that the silicon data show much stronger funneling for heavy-ion bombardment than do the gallium arsenide data, and that the screening treatment predicts this difference. This is consistent with our representation of plasma screening as an effect dependent on track conductivity through the skin depth: for a given ionization density, the gallium arsenide plasma has a much higher conductivity than the silicon plasma because of its greater electron mobility, and its screening should be a correspondingly stronger influence. As an illustration of this difference, Tables I and II give the values of the critical screening parameters (τ , L , δ) and the resulting screening factor f_s as functions of junction bias for copper ions incident on gallium arsenide and silicon, respectively.

Table I. Screening parameters for 56.9-MeV Cu ions in GaAs, $N_D = 8.0 \times 10^{14}/\text{cm}^3$

Bias (V)	τ (ns)	δ (μm)	L (μm)	f_s
0	1.94	7.20	5.92	0.44
2	1.11	5.45	7.69	0.24
5	0.58	3.92	7.69	0.14
10	0.35	3.07	7.69	0.08
15	0.28	2.74	7.69	0.06
20	0.25	2.57	7.69	0.05

Table II. Screening parameters for 59.6-MeV Cu ions in n-type Si, $N_D = 2.8 \times 10^{15}/\text{cm}^3$

Bias (V)	τ (ns)	δ (μm)	L (μm)	f_s
0	1.10	13.40	4.89	0.69
2	1.01	12.80	7.85	0.54
5	0.89	12.06	10.16	0.43
10	0.59	9.78	10.16	0.35
15	0.48	8.88	10.16	0.32
20	0.43	8.33	10.16	0.30

In a final note on the gallium arsenide data, we observed pronounced ~ 500 MHz oscillations riding on the expected waveforms. Originally, we attributed them to our test circuit configuration, but after a series of exploratory tests, reported that the oscillations appeared to be produced in the diode. As a result of our recent collaborative investigations of the effect with Z. Shanfield and coworkers of Northrop Research and Technology Center, we now conclude that the oscillations are in fact the consequence of signal ringing in the test circuit.

CONCLUSIONS

We have offered a description of the funnel mechanism for the transiently isolated junction. The plasma screening adjustment to the McLean-Oldham effective funnel length model has been shown to give reasonably accurate predictions of prompt charge collection in both silicon and gallium arsenide diodes, for both light- and heavy-ion bombardments. The results of this study further suggest that plasma screening should be a much stronger effect in gallium arsenide than in silicon; one would therefore expect correspondingly smaller prompt charge collections in gallium arsenide devices struck by heavy ions.

ACKNOWLEDGEMENTS

The authors wish to thank T. R. Oldham, F. B. McLean, and J. M. McGarrrity of Harry Diamond Laboratories, and J. G. Brennan of The Catholic University of America for helpful technical discussions, and A. R. Knudson of the Naval Research Laboratory for the loan of the vacuum test chamber used in the heavy-ion experiments on gallium arsenide.

REFERENCES

1. C. M. Hsieh, P. C. Murley, and R. R. O'Brien, *IEEE El. Dev. Lett.* **EDL-2**, 103 (1981).
2. C. M. Hsieh, P. C. Murley, and R. R. O'Brien, *Proc. of IEEE Int'l Reliability Phys. Symposium*, Orlando, Florida, April 7, 38 1981.
3. C. M. Hsieh, P. C. Murley, and R. R. O'Brien, *IEEE Trans. El. Dev.*, **ED-30**, No. 6, 686 (1983).
4. C. Hu, *IEEE El. Dev. Lett.*, **EDL-3**, 31 (1982).
5. G. C. Messenger, *IEEE Trans. Nucl. Sci.* **NS-29**, 2024 (1982).
6. F. B. McLean and T. R. Oldham, *IEEE Trans. Nucl. Sci.*, **NS-29**, 2018 (1982).
7. T. R. Oldham and F. B. McLean, *IEEE Trans. Nucl. Sci.*, **NS-30**, 4493 (1983).
8. R. M. Gilbert, G. K. Ovrebo, J. Schifano, and T. R. Oldham, *IEEE Trans. Nucl. Sci.* No. 6, **NS-31**, 1570 (1984).
9. H. L. Grubin, J. P. Kreskovsky, and B. C. Weinberg, *IEEE Trans. Nucl. Sci.*, **NS-31**, No. 6, 1161 (1984).
10. M. A. Hopkins and J. R. Srouf, *IEEE Trans. Nucl. Sci.*, **NS-30**, No. 6, 4457 (1983).
11. T. R. Oldham, private communication.
12. J. F. Ziegler, *Handbook of Stopping Cross-Sections for Energetic Ions in all Elements*, Pergamon Press, Inc. (1980).
13. B. G. Streetman, *Solid State Electronic Devices*, Prentice-Hall, Inc., 423 (1980).